Korean J. Chem. Eng., 34(4), 1214-1221 (2017)
DOI: 10.1007/s11814-016-0354-5

pISSN: 0256-1115
eISSN: 1975-7220

Pyrolysis kinetic analysis of poly(methyl methacrylate) using evolved gas analysis-mass spectrometry

Tae Uk Han*,‡, Young-Min Kim*,,‡, Atsushi Watanabe**, Norio Teramae**,***, Young-Kwon Park****, and Seungdo Kim*,†**

*Department of Environmental Sciences and Biotechnology, Hallym University, Chuncheon 24252, Korea
**Frontier Laboratories Ltd., 4-16-20, Saikon, Koriyama, Fukushima 963-8862, Japan
***Department of Chemistry, Graduate School of Science, Tohoku University, Aoba-ku, Sendai 980-8578, Japan
****School of Environmental Engineering, University of Seoul, Seoul 02504, Korea
(*Received 14 October 2016 • accepted 17 December 2016*)

Abstract−The results of evolved gas analysis-mass spectrometry (EGA-MS) analysis were used for the kinetic analysis of poly-methyl methacrylate (PMMA) pyrolysis for the first time. Various kinetic methods, such as model-free, integral master-plots, and model-fitting methods, have been applied to derive the kinetic parameters (activation energy, pre-exponential factor and reaction model). The PMMA pyrolysis reaction mechanism was suggested to occur via a single step unzipping reaction producing methyl methacrylate (MMA) as the main pyrolyzate from the kinetic analysis results and mass spectrum obtained from the EGA-MS measurements. The kinetic parameters derived from model-free method combined with the integral master-plots method were comparable to those obtained from the peak property method (PPM). The theoretical curve derived from the kinetic results by the PPM was also well matched with the experimental thermal conversion curve using the EGA-MS measurements.

Keywords: PMMA, EGA-MS, Kinetic Analysis, Reaction Model, Py-GC/MS

INTRODUCTION

Growth of the global population and industrial activity has led to the depletion of fossil fuels and an enormous amount of municipal solid waste (MSW) production worldwide. Accordingly, many countries have focused on the appropriate treatment of MSW and the production of renewable energy [1,2].

Pyrolysis, a thermochemical technique, can be a promising option for combustible wastes and/or biomass to renewable energy [3-9]. Therefore, it can meet both concepts: (1) waste management and (2) energy recovery from waste. Waste plastics are a valuable resource to apply the pyrolysis process owing to their physico-chemical properties (high volatile, low sulfur and nitrogen, and high calorific value). With the continuous growth of the plastics market, global plastic production was 299 million tons in 2013 [5]. As expected, the amount of waste plastic is also increasing gradually. In Europe, approximately 62% (total amount 25 million ton $year^{-1}$) of waste plastic is recycled and used for energy recovery as a resource [10]. On the other hand, many countries still have a higher percentage of plastic waste sent to landfills than the average percentage of landfills (38%) in Europe except for countries with a landfill ban on waste plastic [10]. Poly-methyl methacrylate (PMMA) is a thermoplastic. Owing to its high transparency, weather resistance, etc., it is used in many fields as the parts in the car industry as well as in electronic and electrical equipment, construction materials, etc. [11]. Compared to other polyolefin plastics, PMMA exhibits different thermal behavior. The pyrolysis reaction of PMMA involves a radical and unzipping reaction that uniformly produces methyl methacrylate (MMA) monomer as the main pyrolyzate [12,13]. According to the merit of the recovery feedstock, PMMA pyrolysis has attracted considerable attention, and many studies have been conducted for the recovery of MMA from PMMA using molten metal baths [14], fluidized bed reactor [12], and conical spouted bed reactor [13].

Pyrolysis research fields can be divided into kinetic analysis and product characterization. Thermogravimetric analysis (TGA) is normally used for the pyrolysis kinetic studies of solid materials. The thermal decomposition pattern as a function of temperature and/or time, kinetic parameters for the pyrolysis reaction of polymeric materials can be estimated using TGA [15,16].

Although TGA provides considerable thermal and kinetic information on pyrolysis reactions, many researchers have been eager to explain the pyrolysis reaction in addition to the qualitative information. Therefore, many types of TGA instruments are coupled directly to chemical analysis instruments, such as mass spectrometry (MS) and Fourier transform infrared (FT-IR) spectroscopy [17-20]. On the other hand, the large amount of sample required for stable TGA (~10 mg) can cause saturation or severe contamination of the MS or FT-IR spectroscope when TGA is coupled directly to MS or FT-IR spectroscope without a proper dilution device [21]. On the other hand, a small amount of sample for direct MS analysis (normally below 0.5 mg) does not provide sufficient sensitivity of the TGA balance resulting in an unstable and noisy derivative TG (DTG) curve.

Recently, comparable DTG and evolved gas analysis-MS (EGA-

†To whom correspondence should be addressed.
E-mail: sdkim@hallym.ac.kr
‡Co-first author

MS) curves were obtained from the non-isothermal pyrolysis of polymeric materials, such as printed circuit boards [22,23], pine nut shell [24], *citrus* peel [25] and wood [26]. Although similar curve shapes between DTG and EGA-MS curves were obtained, the kinetic parameters and thermal profiles of pyrolyzates were derived from the DTG results using TGA and EGA-MS results using a pyrolyzer-gas chromatography/MS (Py-GC/MS), respectively. Shiono et al. [21] compared the DTG and EGA-MS curves for fifteen kinds of synthetic polymers and found similar thermal curves between the DTG and EGA-MS curves.

The above comparison results between the DTG and EGA-MS curve suggest that the EGA-MS curve also can be used for the kinetic analysis of a solid pyrolysis reaction if the EGA-MS curve can be converted to the thermal conversion (TC) and derivative TC (DTC) curves, such as the TG and DTG curves obtained from TGA. In this case, both the kinetic analysis and detailed product characterization of pyrolysis reactions can be achieved using a one-instrumentation system. Despite this, there are no reports of kinetic analysis using the EGA-MS results.

We performed kinetic analysis of the non-isothermal pyrolysis of PMMA to determine the pyrolysis reaction parameters and model. EGA-MS measurements were also used instead of TGA to check the feasibility of using the EGA-MS results as the raw data for kinetic analysis. Various kinetic analysis methods, such as model-free, integral master-plots, and model-fitting method were applied to check the reliability of the new kinetic approach.

EXPERIMENTAL

1. Materials

The pellet form of PMMA (LG chemicals, weight-average molecular weight: 100,000 g/mol), which was composed of 97.5% MMA and 2.5% methyl acrylate (MA), was cryo-milled in liquid nitrogen using a milling machine. To minimize the heat- and mass-transfer effect during the experiment, the sample was sieved to make a particle size of less than 500 μm.

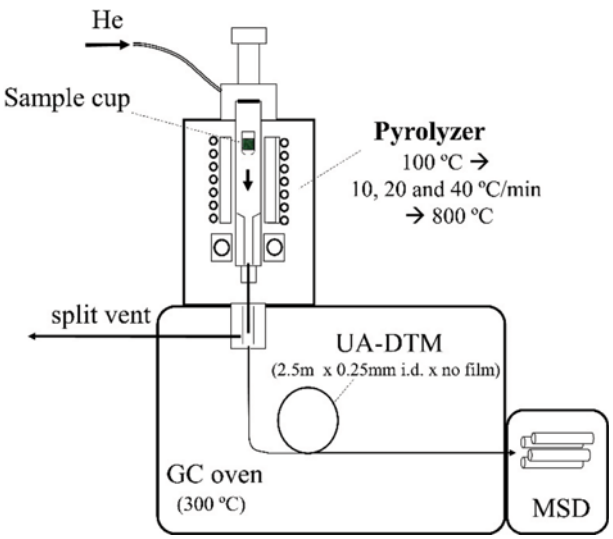

Fig. 1. Schematic flow diagram of Py-GC/MS for EGA-MS measurement.

2. EGA-MS Analysis

For the EGA-MS measurements, a multi-shot pyrolyzer (EGA/Py-3030D, Frontier Laboratories Ltd., Japan) directly attached to the GC/MS (7890A/5975C inert, Agilent Technologies, USA) system was used. Fig. 1 shows a schematic diagram of the Py-GC/MS system for EGA-MS analysis. 0.5±0.05 mg sample of PMMA, loaded at a deactivated sample cup, was dropped into the pyrolyzer furnace at 100 °C and then heated from 100 °C to 800 °C at three linear heating rates of 10, 20, and 40 °C/min under a helium atmosphere. Only 2% of the emission gas from the sample cup was transferred to the MS via a deactivated metal transfer tube (UA-DTM-2.5N, 2.5 m×0.15 mm i.d., Frontier Laboratories Ltd., Japan) using the high split ratio (50 : 1) of the GC inlet. To avoid any condensation or separation of vaporized gas among the systems, the temperatures of the GC inlet, GC oven, and MS interface were maintained at 300 °C. The widest MS scan range (*m/z*: 10~800) was chosen to detect as many of the emission compounds as possible.

3. Kinetic Analysis with EGA-MS Data

The general kinetic equation of a solid-state reaction can be written as follows:

$$\beta(d\alpha/dT)=kf(\alpha)=A\cdot\exp(-E_a/RT)f(\alpha) \quad (1)$$

where β is the linear heating rate (°C/min), k is the reaction constant that depends on the absolute temperature, T, according to the Arrhenius equation, and $f(\alpha)$ is a reaction model that can take a variety of mathematical forms. Herein, A is the frequency factor (min^{-1}), E_a is the activation energy (J/mol), and R is the gas constant (8.314 J/mol·K).

Normally, a reaction conversion fraction (α) is expressed as the sample weight measured by the balance during TGA as follows:

$$\alpha=(M_0-M)/(M_0-M_f) \quad (2)$$

where M_0 is the initial mass, M_f is the mass of residual char, and M is the sample mass during pyrolysis at a certain temperature, T. On the other hand, kinetic analysis using EGA-MS needs to define the conversion term because the EGA-MS curve is expressed as the MS intensity with respect to temperature. Therefore, the reaction conversion fraction-derived EGA-MS results can be expressed as Eq. (3).

$$\alpha=\frac{AMI_T}{AMI_{final}} \quad (3)$$

where AMI_T is the accumulated MS intensity from the initial to certain temperature, AMI_{final} is the accumulated MS intensity from the initial to the final temperature. Fig. 2 shows the conversion procedure from the EGA-MS curve (Fig. 2(a)) to the TC curve (Fig. 2(b)). If the reaction TC curve versus temperature is obtained, the DTC curve (Fig. 2(c)) can also be derived by simple differentiation.

Representative non-isothermal kinetic analysis of the pyrolysis reaction can be divided into model-free and model-fitting methods. We obtained the kinetic parameters of PMMA pyrolysis using a combined model-free method (Flynn-Wall-Ozawa method) [27] with an integral master-plots (IMPs) method [28,29], and model-fitting methods (peak property method [30,31] and Freeman and

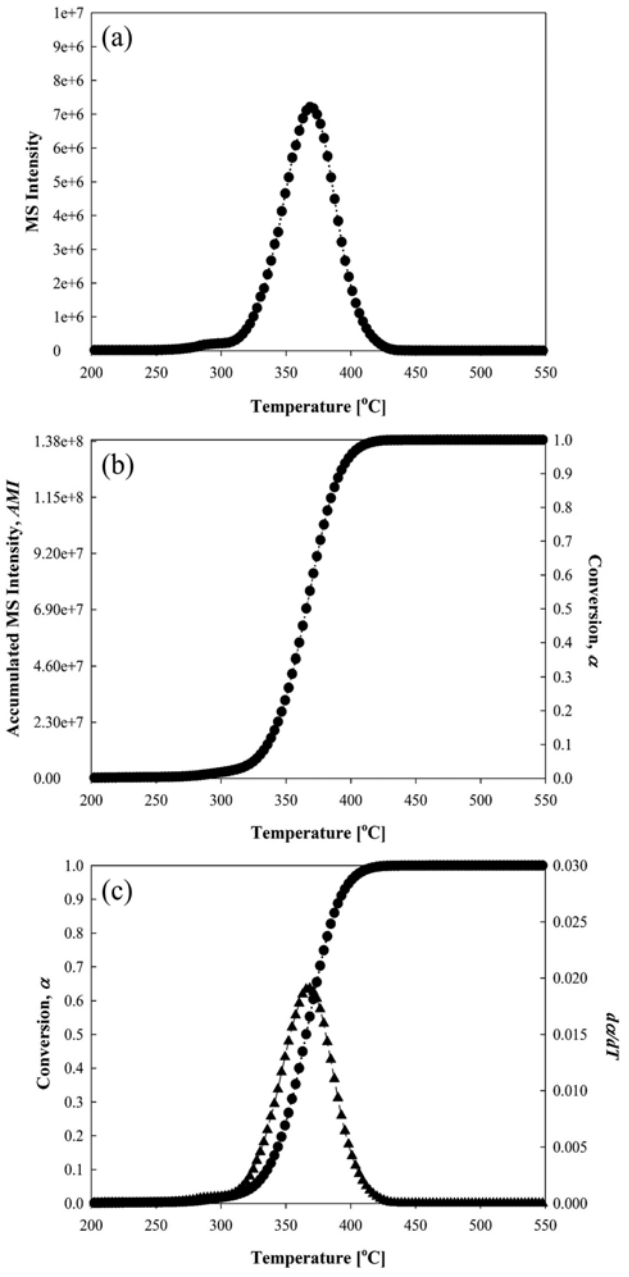

Fig. 2. Converting total ion thermogram (TIT) of PMMA recorded by EGA-MS system to thermal conversion (TC) and derivative TC (DTC) curve via integrating mass intensity.

Carroll method [32]). Each method is explained in the following subchapters. Fig. 3 shows the simplified procedure for the kinetic approach used in this study.

3-1. Model-free Method

The Flynn-Wall-Ozawa (FWO) method [27] was applied to determine the activation energy without the assumption of a reaction model. The Flynn-Wall-Ozawa (FWO) method can be derived as follows: Eq. (4) can be derived from Eq. (1) by rearranging and integrating.

$$g(\alpha)=\int_0^{\alpha}\frac{d\alpha}{f(\alpha)}=\frac{A}{\beta}\int_0^{T}\exp\left(-\frac{E_a}{RT}\right)dT=\left(\frac{AE_a}{\beta R}\right)P(u) \tag{4}$$

Here, u is E_a/RT and there is no analytical solution for P(u) ($-\int_{\infty}^{u}\frac{\exp(-u)}{u^2}du$). Therefore, P(u) was assumed by applying Doyle's approximation in the FWO method, and the final equation (Eq. (5)) can be then written in the following form:

$$\ln(\beta)=-1.502\frac{E_a}{RT}+\left[\ln\left(\frac{AE_a}{R}\right)-5.3305-\ln g(\alpha)\right] \tag{5}$$

Herein, the activation energy at each conversion can be concluded by the slope of the linear representation of $\ln(\beta)$ versus 1/T at each conversion.

3-2. Integral Master-plots Method

The pre-exponential factor is difficult to determine by the FWO method without the assumption of a pyrolysis reaction model. Therefore, we also applied the IMPs method [28,29] in this study to determine the pre-exponential factor together with the reaction model using the predetermined average value of the activation energy derived from the FWO method. The determination of the reaction model by the IMPs method can be explained as follows:

Eq. (4) can be expressed as Eq. (6) by setting the conversion 0.5 as the reference point.

$$g(0.5)=\left(\frac{AE_a}{\beta R}\right)P(u_{0.5}) \tag{6}$$

By dividing Eq. (4) by Eq. (6), final equation of the IMPs method can be expressed as below, where $g(\alpha)$ is the integral form of reaction model.

$$\frac{g(\alpha)}{g(0.5)}=\frac{P(u)}{P(u_{0.5})} \tag{7}$$

The kinetic model of PMMA pyrolysis can be derived by com-

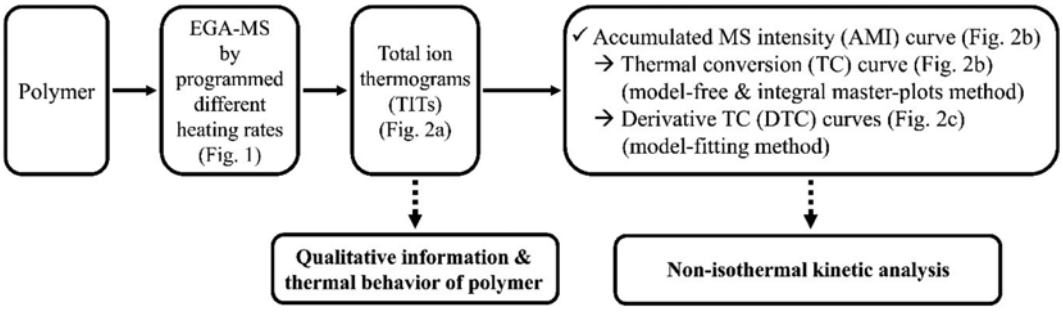

Fig. 3. Simplified procedure of new kinetic approach using EGA-MS.

Table 1. Kinetic models for employed to describe the solid state reaction

Reaction model	Symbol	Differential form f(α)	Integral form g(α)
n-Order	F_n	$(1-\alpha)^n$	$[1/(n-1)][(1-\alpha)^{1-n}-1]$ (n≠1)
First-order	F_1	$1-\alpha$	$-\ln(1-\alpha)$
Second-order	F_2	$(1-\alpha)^2$	$(1-\alpha)^{-1}-1$
Third-order	F_3	$(1-\alpha)^3$	$[(1-\alpha)^{-2}-1]/2$
One-way transport	D_1	0.5α	α^2
Two-way transport	D_2	$[-\ln(1-\alpha)]^{-1}$	$\alpha+(1-\alpha)\ln(1-\alpha)$
Three-way transport	D_3	$1.5(1-\alpha)^{2/3}[1-(1-\alpha)^{1/3}]^{-1}$	$[1-(1-\alpha)^{1/3}]^2$
Ginstling-Brounshtein euaqtion	D_4	$1.5[(1-\alpha)^{1/3}-1]^{-1}$	$(1-2\alpha/3)-(1-\alpha)^{2/3}$
One dimension	R_1	1	α
Two dimensions	R_2	$2(1-\alpha)^{1/2}$	$1-(1-\alpha)^{1/2}$
Three dimensions	R_3	$3(1-\alpha)^{2/3}$	$1-(1-\alpha)^{1/3}$
Two-dimensional	A_2	$2(1-\alpha)[-\ln(1-\alpha)]^{1/2}$	$[-\ln(1-\alpha)^{1/2}]$
Three-dimensional	A_3	$3(1-\alpha)[-\ln(1-\alpha)]^{2/3}$	$[-\ln(1-\alpha)^{1/3}]$
Power law, n=1/2	P_2	$2\alpha^{1/2}$	$\alpha^{1/2}$
Power law, n=1/3	P_3	$3\alpha^{2/3}$	$\alpha^{1/3}$
Power law, n=1/4	P_4	$4\alpha^{3/4}$	$\alpha^{1/4}$

paring the theoretical integral master-plots (g(α)/g(0.5)) for different reaction models (Table 1) and experimental master plots (P(u)/P($u_{0.5}$)) obtained from the EGA-MS data at each heating rates. The residual sum of the squares (S^2), Eq. (8), was applied to prove the goodness of fit of the theoretical plot [33].

$$S^2=\frac{1}{N-1}\left(\Sigma_{i=1}^{N}\frac{g(\alpha_i)}{g(0.5)}-\frac{P(u_i)}{P(u_{0.5})}\right)^2 \quad (8)$$

3-3. Model-fitting Method

Two model-fitting methods, peak property method (PPM) [30, 31] and Freeman and Carroll (FC) method [32], were also used to validate the kinetic parameters derived from FWO and IMPs method. Both can provide the activation energy, pre-exponential factor, and reaction order (n) from derivative conversion and/or conversion curve at a single heating rate.

RESULTS AND DISCUSSION

1. EGA-MS Curve and Mass Spectrum of PMMA Pyrolysis

Fig. 4 shows the TC and DTC curves of PMMA as function of temperature obtained from the EGA-MS analysis of PMMA at different heating rates of 10, 20, and 40 °C/min. As shown in Fig. 4(a), PMMA decomposition was initiated at approximately 300 °C and decomposed rapidly in the narrow temperature range between 300 °C to 400 °C. Therefore, the DTC curves of PMMA (Fig. 4(b)) showed a single predominant peak at each heating rate. Ferriol et al. [34] reported that the average molecular weight is a key factor of the decomposition patterns of PMMA. They showed that the PMMA manufactured by the free radical method usually had four decomposition stages; however, PMMA with a lower molecular weight degrades in two steps due to the structural differences. Kang et al. [12] and Lopez et al. [13] also observed a single predominant peak at the derivative conversion curve of PMMA pyrolysis and reported that a low temperature the decomposition step is negligible compared to the main weight loss step. This same trend of the pyrolysis PMMA behavior was attributed to a number of weak

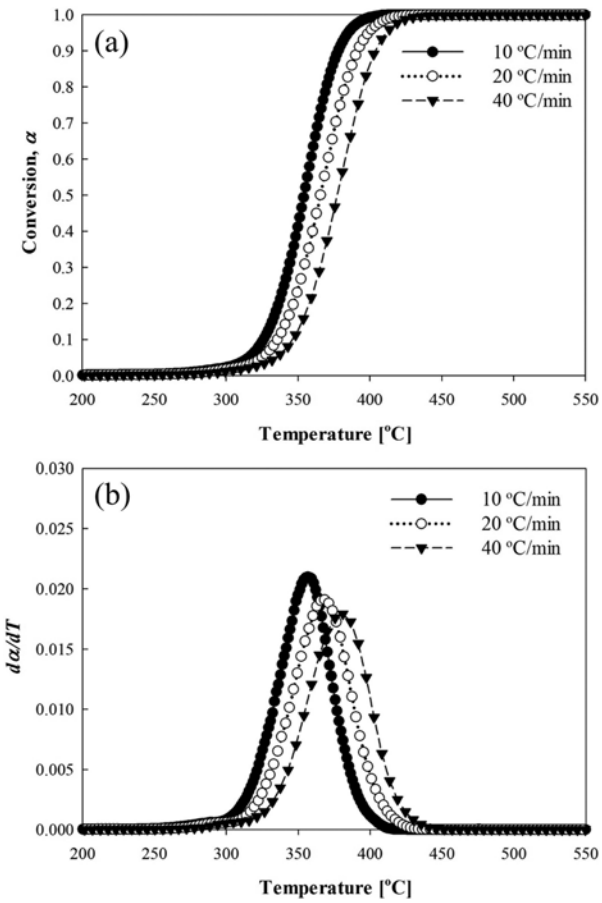

Fig. 4. (a) TC and (b) DTC curves of PMMA at heating rates of 10, 20, and 40 °C/min.

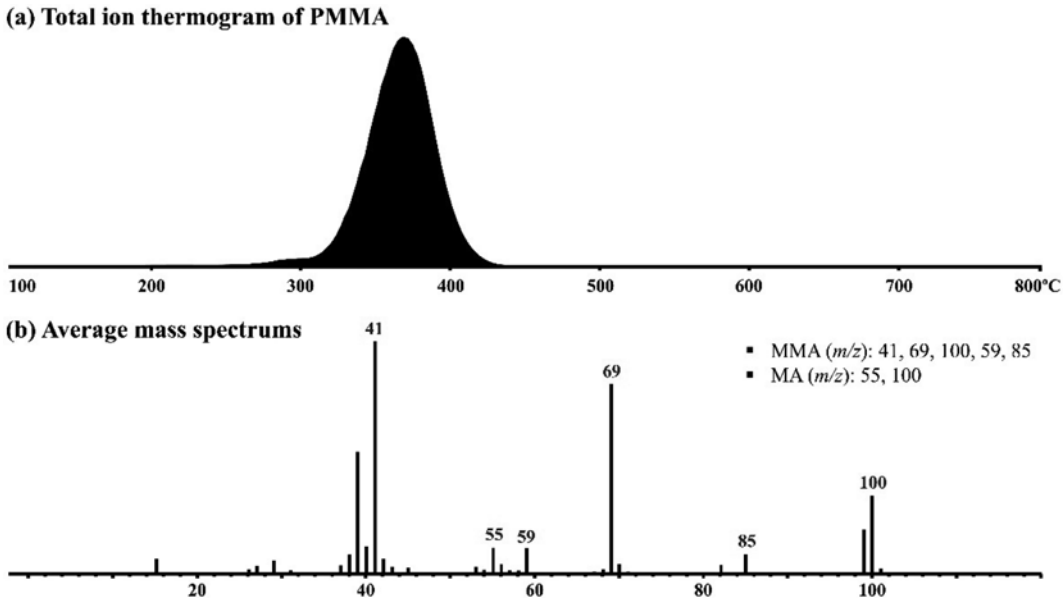

Fig. 5. (a) Total ion thermogram of PMMA at a heating rate of 20 °C/min. (b) Average mass spectrum of TIT.

head-to-head linkage (H-H) and terminal groups, which decomposed mainly at lower temperatures [35-39]. This suggests that the PMMA used in this research has a low molecular weight and small amounts of thermally unstable groups.

The main weight loss step is normally considered to be the random scission of pyrolysis PMMA; thus, the PMMA monomer (MMA) was produced uniformly via an unzipping reaction [12, 13,34]. Fig. 5 shows the EGA-MS curve (Fig. 5(a)) and its average mass spectrum (Fig. 5(b)) of PMMA at a heating rate of 20 °C/min. As expected, the average mass spectrum consisted mainly of the specific ions of MMA (*m/z* 45, 69, 100, 59, 85) together with a minor intensity of MA. This confirmed that MMA was produced mainly by an unzipping reaction. The small amount of MA formation can be explained by the presence of MA as a co-feeding monomer with MMA [12,13].

2. Model-free Kinetic Analysis

Fig. 6 shows the lnβ vs. 1/T plots for different conversions obtained from the EGA-MS analysis of PMMA. The high linearity of the plots, R^2>0.999 at all conversions, indicates the reliability of FWO kinetic analysis using the EGA-MS data. The apparent activation energies obtained from the FWO method (Fig. 7) decreased gradually with increasing conversion in the range, 202.6 and 186.4 kJ/mol. The average apparent activation energy was 193.0 kJ/mol. Hu et al. [39] examined the pyrolysis behaviors of five types of PMMA and considered two steps in the thermal decomposition of PMMA depending on the different terminal group. They reported that the mean activation energies of all PMMA samples in the second step (the scission of main chain) were close to each other, ranging from 210-220 kJ/mol. Holland and Hay [40] also reported similar activation energies (210±10 kJ/mol) for the pyrolysis of PMMA. Although both used the TGA results for the kinetic analysis of PMMA, the resulting activation energies were comparable to those obtained in the present study using the EGA-MS results. This highlights the

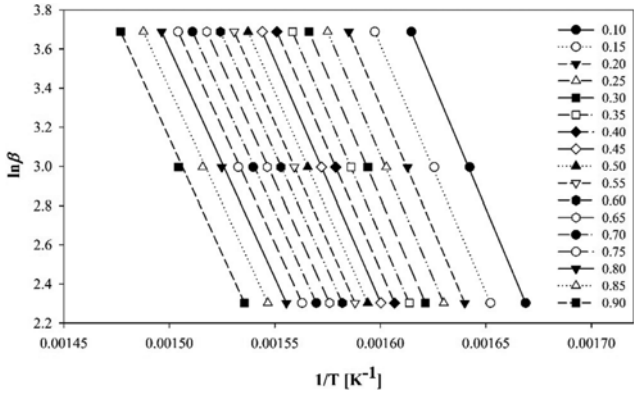

Fig. 6. Flynn-Wall-Ozawa plots for lnβ versus 1/T as a function of conversion.

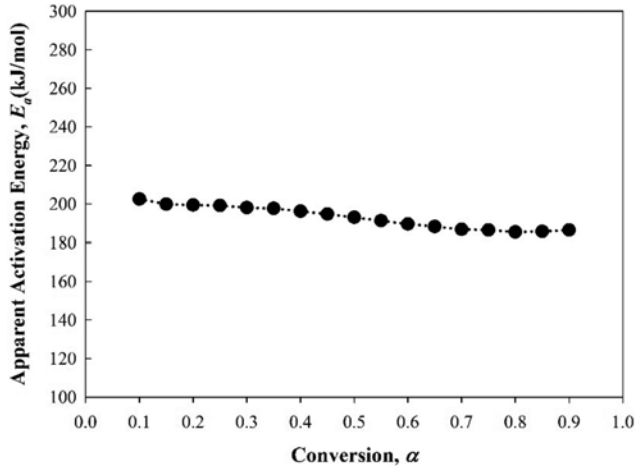

Fig. 7. Calculated apparent activation energies at different conversions of PMMA.

feasibility of the FWO method with EGA-MS analysis as a kinetic analysis tool.

Even if the pyrolysis reaction follows a random scission process, the reaction can be divided into two different pathways, (1) a single step reaction and (2) multi-step reaction, according to the variation pattern of the activation energy [41]. Wanjun et al. [41] suggested that the phenomenon of a single step reaction is independent of the activation energy as a function of conversion. In addition, a multi-step reaction tends to have variation patterns of the activation energy depending on the degree of conversion. As a result, PMMA pyrolysis can be explained as a single step reaction handled by a random scission pathway because the activation energies are distributed in a narrow range between 186.4 and 202.6 kJ/mol without a sudden change at all conversions.

3. Integral Master-plots Analysis

Although the reaction model of a single step reaction is generally assumed to be *n*-order (especially n=1), the assumption of an improper model can lead to an incorrect pre-exponential factor (A) [33]. Therefore, the IMPs method was also conducted to determine the pyrolysis reaction model and pre-exponential factor (A) of the PMMA in this study.

For IMPs analysis, P(u) can be calculated using Doyle's approximation (P(u)=0.00484·exp(−1.0516u)) using the mean activation energy (193.0 kJ/mol) derived from the FWO method. Fig. 8 illustrates the theoretical integral master-plots (Table 1) and experimental master-plots against α. The experimental curves were folded excellently with the theoretical one corresponding to the $F_{1.3}$ model, $g(\alpha)=((1-\alpha)^{-0.3}-1)/0.3$. The mean value of S^2 for the $F_{1.3}$ model was 0.00187, which was lower than other *n*-order plots ($F_{1.1}$=0.03905, $F_{1.2}$=0.01124, and $F_{1.4}$=0.01869). This suggests that the $F_{1.3}$ model can be used to simulate the PMMA pyrolysis reaction.

Ferriol et al. [34] also reported that the reaction order of PMMA pyrolysis was 1.1-1.3 for the main chain scission with respect to the heating rates. In addition, Holland et al. [40] concluded that the reaction order of PMMA pyrolysis was 1.0-1.2 with respect to conversion. Kang et al. [12] also estimated the kinetic parameters using the FC method and concluded that the reaction order was 1.43. Through previous studies [12,34], it is expected that different kinetic parameters (E and A) could be obtained due to the use of different reaction orders (n). Kim et al. [30] and Eom et al. [31] suggested that the activation energy and pre-exponential factor are governed by the reaction order; thus, an inappropriate reaction order, i.e., reaction model, leads to incorrect kinetic parameters.

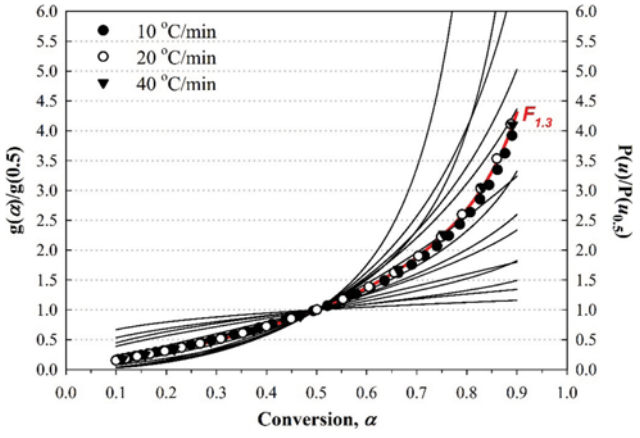

Fig. 8. Comparison between theoretical integral master-plots plots $g(\alpha)/g(0.5)$ for different reaction models (Table 1) and experimental master plots of $P(u)/P(u_{0.5})$ against α from EGA-MS data at heating rates of 10, 20, and 40 °C/min.

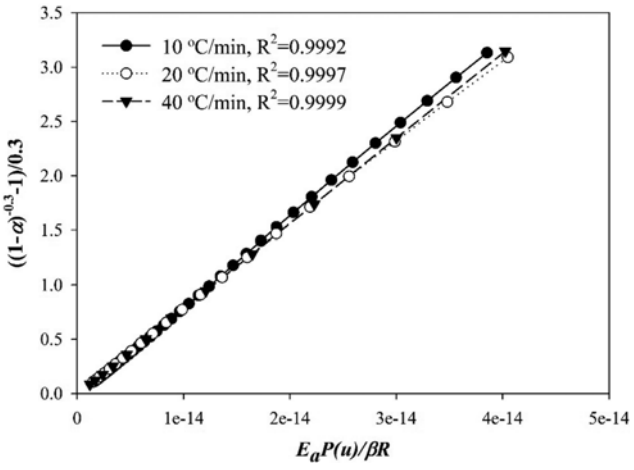

Fig. 9. Plots of $((1-\alpha)^{-0.3}-1)/0.3$ versus $E_aP(u)/\beta R$ from experimental data recorded at heating rates of 10, 20, and 40 °C/min.

Table 2. Kinetic parameters of pyrolysis PMMA obtained from the peak property method (PPM) and Freeman and Carroll (FC) method

	Heating rate (β, °C/min)	Reaction order (n)	Activation energy (E, kJ/mol)	Pre-exponential factor (lnA, A: min^{-1})
PPM	10	1.39	214.5	40.5
	20	1.36	199.2	37.5
	40	1.27	185.9	34.9
	Average	1.34	199.9	37.6
	RSD (%)	4.91	7.17	7.47
FC	10	1.45	216.4	41.1
	20	1.44	206.8	38.8
	40	1.39	205.7	38.2
	Average	1.43	209.6	39.4
	RSD (%)	2.10	2.80	3.80

Although the reaction orders derived from these studies [12,34] were different, all of them insisted on the *n*-order model as the pyrolysis reaction model of PMMA as derived by IMP analysis in this study.

Fig. 9 presents plots of $((1-\alpha)^{-0.3}-1)/0.3$ vs. $E_aP(u)/\beta R$. The slope corresponded to the pre-exponential factor (A, min^{-1}) at each heating rate according to the Eq. (1). The values of lnA for the *n*-order model ($F_{1.3}$) were 32.02, 31.98, and 31.99 (mean 32.00) at heating rates of 10, 20, and 40 °C/min, respectively.

4. Model-fitting Kinetic Analysis

The PPM and FC method are powerful kinetic tools to determine the activation energy (E_a), pre-exponential factor (A), and reaction order (n) if the reaction model is assumed or concluded to be a *n*-order reaction [30-32]. PPM uses the peak property information (peak temperature, peak height and peak conversion) to deliver the kinetic parameters [30,31]. The FC method is a unique method that can determine the kinetic parameters with the TG/DTG results obtained at a single heating rate [32].

Table 2 presents the kinetic parameters derived from the PPM and FC methods. The detailed peak properties are shown in Table 3. The mean values of the reaction order, activation energy, and lnA of PMMA pyrolysis derived by the PPM method were 1.34 (n), 199.9 kJ/mol, and 37.6 (lnA: min^{-1}), respectively. Compared to the kinetic parameters obtained from the FC method, all the values estimated by PPM were lower than those of the FC method and comparable to those derived by FWO combined with the IMPs methods. To verify the kinetic results obtained from model-fitting methods, Fig. 10 compares the experimental derivative conversion curves with the theoretical curves. As shown in Fig. 10, the theoretical curve derived from the PPM results showed a more duplicated experimental curve than that of the FC method, suggesting that the PPM matched up with the result of the FWO and IMPs method. This also suggests that the EGA-MS results can be used for kinetic analysis using model-free and model-fitting methods.

Table 3. Three peak properties of derivative conversion of PMMA at heating rates of 10, 20, and 40 °C/min

Heating rate (β, °C/min)	Peak temperature (T_m, °C)	Peak height (H_m, $d\alpha/dT$)	Peak conversion (α_m)
10	356.61	0.021	0.5498
20	368.36	0.019	0.5523
40	381.00	0.018	0.5651

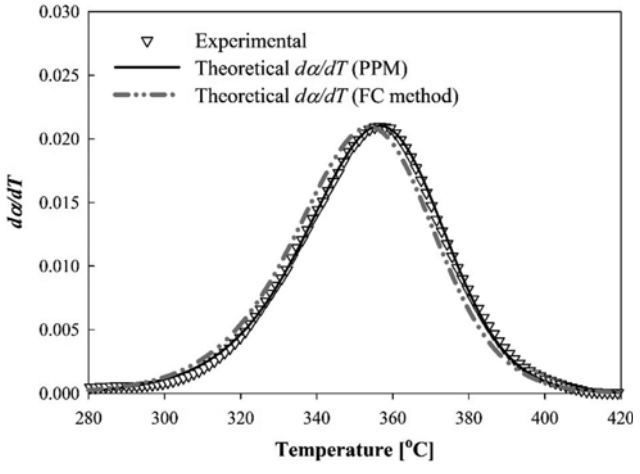

Fig. 10. Comparison of experimental DTC curve at a heating rate 20 °C/min with theoretical ones derived from PPM and FC method.

CONCLUSION

EGA-MS measurements were used as a kinetic analysis tool for the pyrolysis of PMMA instead of TGA. To validate this analytical approach, traditional kinetic analysis methods, such as model-free, IMPs, and model-fitting methods were applied to the non-isothermal kinetic analysis of PMMA pyrolysis to determine its activation energy (E_a), reaction model (f(x)), and pre-exponential factor (A). The mean mass spectrum of the EGA thermogram and model-free kinetic analysis results showed that the PMMA pyrolysis reaction is a single step unzipping reaction producing the MMA monomer as the main pyrolyzate with an average E_a value of 193 kJ/mol. The *n*-order (especially, n=1.3 with lnA=32.0) reaction is represented as the PMMA pyrolysis model via the IMPs method. The kinetic parameters derived from the model-fitting kinetic analysis results were also comparable to those obtained by model-free combined with IMPs methods. Between the two model-fitting methods, the theoretical derivative thermal conversion (DTC) curve constructed by the kinetic parameters (n=1.34, average E_a=199.9 kJ/mol, and lnA=37.6) derived from the peak property method simulated the experimental DTC curve better than those (n=1.43, average E_a=209.6 kJ/mol, and lnA=39.4) derived from the FC method.

ACKNOWLEDGEMENTS

This research was supported by Hallym University Research Fund, 2016 (HRF-201607-012).

REFERENCES

1. J. Hong, Y. Chen, M. Wang, L. Ye, C. Qi, H. Yuan, T. Zheng and X. Li, *Renew. Sustainable Energy Rev.*, **69**, 168 (2017).
2. T. F. Astrup, D. Tonini, R. Turconi and A. Boldrin, *Waste Manage.*, **37**, 104 (2015).
3. D. Chen, L. Yin, H. Wang and P. He, *Waste Manage.*, **34**, 2466 (2014).
4. T. Kan, V. Strezov and T. J. Evans, *Renew. Sustainable Energy Rev.*, **57**, 1126 (2016).
5. S. D. A. Sharuddin, F. Abnisa, W. M. A. W. Daud and M. K. Aroua, *Energy Convers. Manage.*, **115**, 308 (2016).
6. H. Lee, Y.-M. Kim, I.-G. Lee, J.-K. Jeon, S.-C. Jung, J. D. Chung, W. G. Choi and Y.-K. Park, *Korean J. Chem. Eng.*, **33**, 3299 (2016).
7. E. H. Lee, R.-S. Park, H. Kim, S.-H. Park, S.-C. Jung, J.-K. Jeon, S. C. Kim and Y.-K. Park, *J. Ind. Eng. Chem.*, **37**, 18 (2016).
8. S. H. Park, H. J. Cho, C. Ryu and Y.-K. Park, *J. Ind. Eng. Chem.*, **36**, 314 (2016).
9. J. S. Cha, S. H. Park, S.-C. Jung, C. Ryu, J.-K. Jeon, M.-C. Shin and Y.-K. Park, *J. Ind. Eng. Chem.*, **40**, 1 (2016).
10. Association of Plastic Manufacturers Europe, An analysis of Euro-

pean plastics production, demand and waste data, Belgium: European Association of Plastics recycling and Recovery Organisations, 1-34 (2015).
11. Poly(methyl methacrylate), http://en.wikipedia.org/wiki/Poly(methyl_methacrylate) (Accessed 12.10.2016).
12. B.-S. Kang, S. G. Kim and J.-S. Kim, *J. Anal. Appl. Pyrol.*, **81**, 7 (2008).
13. G. Lopez, M. Artetxe, M. Amutio, G. Elordi, R. Aguado, M. Olazar and J. Bilbao, *Chem. Eng. Process.*, **49**, 1089 (2010).
14. J. Domingo and D. Cabanero, *Spanish Patent*, **192909** (1945).
15. Y.-M. Kim, H. W. Lee, S.-H. Lee, S.-S. Kim, S. H. Park, J.-K. Jeon, S. Kim and Y.-K. Park, *Korean J. Chem. Eng.*, **28**, 2012 (2011).
16. P. E. Sanchez-Jimenez, L. A. Perez-Maqueda, A. Perejon and J. M. Criado, *Thermochim. Aata*, **552**, 54 (2013).
17. M. Calle, H. J. Jo, C. M. Doherty, A. J. Hill and Y. M. Lee, *Macromolecules*, **48**, 2603 (2015).
18. R. Wang and Z. Xu, *J. Hazard. Mater.*, **302**, 45 (2016).
19. L. Tian, B. Shen, H. Xu, F. Li, Y. Wang and S. Singh, *Energy*, **103**, 533 (2013).
20. J. Yang, H. Chen, W. Zhao and J. Zhou, *J. Anal. Appl. Pyrol.*, **117**, 296 (2016).
21. A. Shiono, A. Hosaka, C. Watanabe, N. Teramae, N. Nemoto and H. Ohtani, *Polym. Test.*, **42**, 54 (2015).
22. Y.-M. Kim, S. Kim, J.-Y. Lee and Y.-K. Park, *Environ. Eng. Sci.*, **30**, 706 (2013).
23. Y.-M. Kim, T. U. Han, C. Watanabe, N. Teramae, Y.-K. Park, S. Kim and B. Hwang, *J. Anal. Appl. Pyrol.*, **115**, 87 (2015).
24. Y.-M. Kim, S. Kim, T. U. Han, Y.-K. Park and C. Watanabe, *J. Anal. Appl. Pyrol.*, **110**, 435 (2014).
25. Y.-M. Kim, H. W. Lee, S. Kim, C. Watanabe and Y.-K. Park, *Bioenergy Res.*, **8**, 431 (2015).
26. T. U. Han, Y.-M. Kim, C. Watanabe, N. Teramae, Y.-K. Park, S. Kim and Y. Lee, *J. Ind. Eng. Chem.*, **32**, 345 (2015).
27. ASTM E698-11 Standard Test Method for Arrhenius Kinetic Constants for Thermally Unstable Materials Using Differential Scanning Calorimetry and the Flynn/Wall/Ozawa Method.
28. F. J. Gotor, J. M. Criado, J. Malek and N. Koga, *J. Phys. Chem. A*, **104**, 10777 (2000).
29. Z. Shuping, W. Yulong, Y. Mingde, L. Chun and T. Junmao, *Bioresour. Technol.*, **101**, 359 (2010).
30. S. Kim, E.-S. Jang, D.-H. Shin and K.-H. Lee, *Polym. Degrad. Stabil.*, **85**, 799 (2004).
31. Y. Eom, S. Kim, S.-S. Kim and S.-H. Chun, *J. Ind. Eng. Chem.*, **12**, 846 (2006).
32. E. S. Freeman and B. Carroll, *J. Phys. Chem.*, **62**, 394 (1958).
33. S. Kim and Y.-C. Kim, *J. Anal. Appl. Pyrol.*, **73**, 117 (2005).
34. M. Ferriol, A. Gentilhomme, M. Cochez, N. Oget and J. L. Mieloszynski, *Polym. Degrad. Stabil.*, **79**, 271 (2003).
35. T. Kashiwagi, A. Inaba, J. E. Brown, K. Hatada, T. Kitayama and E. Masuda, *Macromolecules*, **19**, 2160 (1986).
36. A. Inaba, T. Kashiwagi and J. E. Brown, *Polym. Degrad. Stabil.*, **21**, 1 (1988).
37. L. E. Manring, *Macromolecules*, **22**, 2673 (1989).
38. L. E. Manring, D. Y. Sogah and G. M. Cohen, *Macromolecules*, **22**, 4652 (1989).
39. Y.-H. Hu and C.-Y. Chen, *Polym. Degrad. Stabil.*, **82**, 81 (2003).
40. B. J. Holland and J. N. Hay, *Thermochim. Acta*, **388**, 253 (2002).
41. T. Wanjun, W. Cunxin and C. Donghua, *Polym. Degrad. Stabil.*, **87**, 389 (2005).